Article:
Shen, J.X., Zhu, Z.Q. and Howe, D. (2002) Improved speed estimation in sensorless PM brushless AC drives. IEEE Transactions on Industry Applications, 38 (4). pp. 1072-1080. ISSN: 0093-9994

https://doi.org/10.1109/TIA.2002.800778

Improved Speed Estimation in Sensorless PM Brushless AC Drives

J. X. Shen, *Member, IEEE*, Z. Q. Zhu, *Senior Member, IEEE*, and David Howe

***Abstract*—The application of flux-observer-based sensorless control to permanent-magnet brushless ac motor drives is described. Current methods of speed estimation are assessed, both theoretically and experimentally, and an improved method, which combines the best features of methods in which speed is derived from the differential of rotor position and from the ratio of the electromotive force to excitation flux linkage, is proposed. Its performance is verified experimentally.**

***Index Terms*—Brushless ac drives, flux observer, permanent-magnet machines, sensorless control, speed estimation.**

I. Introduction

NUMEROUS sensorless control techniques have been proposed for permanent-magnet (PM) brushless ac (BLAC) drives. Basically, however, these can be classified into two categories: 1) those in which speed is estimated from an observer and the rotor position is obtained by integration [1]–[3] and 2) those in which the rotor position is estimated from an observer and the speed is calculated by differentiation [4]–[9]. However, in the first category, inaccuracies in the estimated rotor position may arise due to speed errors, the integration of a constant error, for example, resulting in an unreliable estimate of rotor position unless an appropriate compensating algorithm is employed. Similarly, in the second category, if the speed is derived simply from the differential of rotor position [6], [7], noise will be amplified and lead to errors in the estimated speed.

When the rotor position is deduced directly from the observed flux vector, Lagerquist [10] recommended that the flux vector should be preprocessed with a low-pass filter to improve the accuracy of the derived position signal such that it can be differentiated for the estimation of speed. However, in a variable-speed BLAC drive, the use of a low-pass filter will generally introduce a phase shift to the fundamental flux vector over a wide frequency band. Thus, an average speed method is more widely used, since it gives the correct value when the motor operates at steady state. However, it is not usually used for speed feedback in servo systems, since its dynamic response is generally not fast enough.

Paper IPCSD 02–033, presented at the 2001 IEEE International Electric Machines and Drives Conference, Cambridge, MA, June 17–20, and approved for publication in the IEEE TRANSACTIONS ON INDUSTRY APPLICATIONS by the Industrial Drives Committee of the IEEE Industry Applications Society. Manuscript submitted for review June 23, 2001 and released for publication May 17, 2002.

The authors are with the Department of Electronic and Electrical Engineering, University of Sheffield, Sheffield S1 3JD, U.K. (e-mail: j.x.shen@ieee.org; z.q.zhu@shef.ac.uk; d.howe@shef.ac.uk).

Publisher Item Identifier 10.1109/TIA.2002.800778.

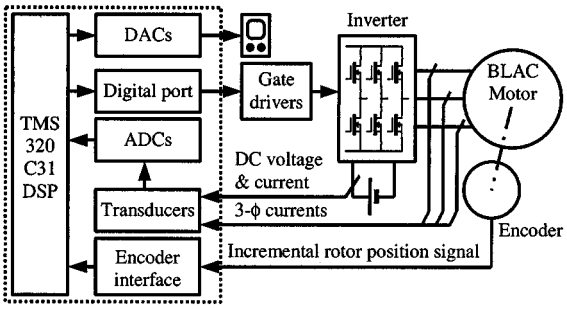

Fig. 1. Block diagram of DSP-controlled BLAC drive system.

An alternative approach, proposed by Watanabe [11] and Matsui [4], [5], is to determine the speed from the ratio of the amplitude of the induced electromotive force (EMF) to the excitation flux linkage. However, while this method of speed estimation has a fast response, it has two significant drawbacks. Firstly, the calculation of the EMF requires the differential of the current. Thus, noise can cause a potentially significant speed error. While Sharkh [12], [13] eliminated the need for the differential, this resulted in a significantly more complex control system design. Kim [14], on the other hand, assumed that the current was constant at the end of each flux observing step, so that its differential was zero. However, in general, such an assumption is not appropriate. Secondly, parameters, such as the winding resistance, inductance, and excitation flux linkage, may vary, due, for example, to variations in temperature and saturation, and cause further errors in the estimated speed. Thus, Kim [14] also compensated for parameter variations, using the estimated average speed as the compensation reference (i.e., input variable). However, it is difficult to compensate for variations in three parameters from only one input variable.

In general, the derivation of the speed from the estimated rotor position results in significant noise. Further, while the estimation of the average speed may be accurate under steady-state operating conditions, it is usually not fast enough to give good dynamic response. In contrast, the estimation of the speed from the induced EMF and excitation flux linkage results in fast dynamic response but low accuracy. Therefore, the development of an improved speed estimation method is of considerable interest.

In this paper, the basic principle of flux-observer-based sensorless control is briefly described, and the performance of an improved speed estimation method, which combines the best features of the foregoing methods, is demonstrated.

The investigation utilizes a TMS320C31 digital-signal-processor (DSP)-based drive as shown in Fig. 1, which supplies a

TABLE I
SPECIFICATION OF BLAC MOTOR

DC voltage:	100 V
Maximum speed:	3000 rpm
Rated torque:	0.6 Nm
Phase resistance:	0.466 ohm
Self-inductance:	3.19 mH
Mutual-inductance:	-1.31 mH
Excitation flux-linkage:	0.0928 Wb

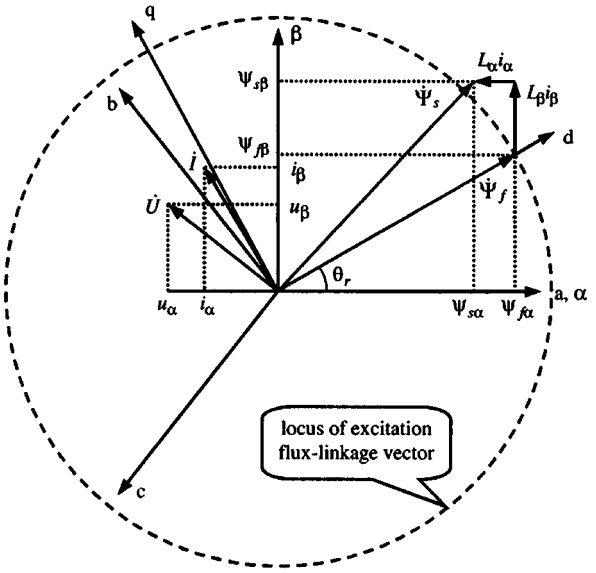

Fig. 2. Phasor diagram of BLAC motor.

two-pole surface-mounted PM BLAC motor. The motor specification is given in Table I. An encoder is used to measure the actual rotor position and to deduce the speed from the differential of position, and these are compared with values obtained from the existing and proposed sensorless techniques.

II. FLUX-OBSERVER-BASED SENSORLESS CONTROL

The phasor diagram of a BLAC motor is shown in Fig. 2, the current vector ($\dot{I}$) and the voltage vector ($\dot{U}$) being derived from measured phase currents, the dc-link voltage and the inverter switching vector, and the transformation matrix from the a–b–c reference frame to the stationary α–β reference frame. The vector $\dot{\Psi}_s$ represents the resultant stator winding flux linkage, while the vector $\dot{\Psi}_f$ represents the excitation flux linkage due to the permanent magnets, which is in phase with the rotor d axis. Hence, the rotor position can be obtained from the estimated phase angle θ_r.

Since

$$\dot{U} = \frac{d\dot{\Psi}_s}{dt} + R \cdot \dot{I} \tag{1}$$

where R is the winding resistance, then $\dot{\Psi}_s$ is observed from

$$\dot{\Psi}_s = \int_0^t \left(\dot{U} - R \cdot \dot{I}\right) dt + \dot{\Psi}_{s(0)}. \tag{2}$$

With zero current in the stator windings, the stator flux-linkage vector is simply the excitation flux-linkage vector, i.e., $\dot{\Psi}_{s(0)} = \dot{\Psi}_f$, which is obtained by initially aligning the rotor before the flux observer is applied.

From Fig. 2, it is seen that $\dot{\Psi}_f$ can be calculated from $\dot{\Psi}_s$, the current vector $\dot{I}$, and winding inductance. Further, if surface-mounted magnets are employed, saliency can be neglected, $L_\alpha = L_\beta = L_s$, and $\dot{\Psi}_f$ is simply calculated from

$$\dot{\Psi}_f = \dot{\Psi}_s - L_s \dot{I}. \tag{3}$$

In the α–β reference frame, $\dot{\Psi}_f$ is expressed by the projections $\psi_{f\alpha}$ and $\psi_{f\beta}$ on the α and β axes, as shown in Fig. 2. Therefore, the rotor position is obtained as

$$\theta_r = \arctan \frac{\psi_{f\beta}}{\psi_{f\alpha}}. \tag{4}$$

Fig. 3(a) shows the locus of the observed flux vector $\dot{\Psi}_f$ for the experimental drive system. As will be seen, while it is almost circular, it is continuously being displaced, due to the integration in (2), which amplifies any dc offset or error in the measured currents until saturation is reached. Clearly, it is not possible to deduce the rotor position from such a changing flux vector locus. Thus, a high-pass filter, having the transfer function $s/(s+\omega_0)$, is applied to the variables to be integrated. Since the transfer function of a pure integrator is $1/s$, the resultant transfer function is $1/(s+\omega_0)$, which is equivalent to replacing the integrator by a low-pass filter [15]. Hence, (2) becomes

$$\dot{\Psi}_s = \int_0^t \left[-\omega_0 \dot{\Psi}_s + \left(\dot{U} - R \cdot \dot{I}\right)\right] dt + \dot{\Psi}_{s(0)}. \tag{5}$$

With the cutoff frequency ω_0 in the experimental drive set at 9.4 rad/s, the circular locus of the observed flux vector $\dot{\Psi}_f$ remains stable, as shown in Fig. 3(b). The estimated rotor position and the actual position, expressed in terms of the encoder resolution of 4000 pulses per revolution, are compared in Fig. 3(c), the maximum difference being 50 pulses, or 4.5° electrical, which is sufficiently accurate for the vector control of most servo drives.

III. SPEED ESTIMATION FROM DIFFERENTIAL OF ROTOR POSITION

The rotor angular velocity ω_p is given by

$$\omega_p = \frac{d\theta}{dt} \approx \frac{\theta_{r(k)} - \theta_{r(k-1)}}{\Delta t_s} \tag{6}$$

where $\theta_{r(k-1)}$ and $\theta_{r(k)}$ are the instantaneous rotor positions at the start and end of the kth time interval Δt_s, respectively. Since, in general, errors will exist in $\theta_{r(k-1)}$ and $\theta_{r(k)}$, then

$$\begin{aligned}\omega_p &= \frac{\left(\theta_{r\_\text{actual}(k)} - \theta_{r\_\text{error}(k)}\right) - \left(\theta_{r\_actual(k-1)} - \theta_{r\_\text{error}(k-1)}\right)}{\Delta t_s} \\ &= \frac{\left(\theta_{r\_\text{actual}(k)} - \theta_{r\_\text{actual}(k-1)}\right) - \left(\theta_{r\_\text{error}(k)} - \theta_{r\_\text{error}(k-1)}\right)}{\Delta t_s} \\ &= \frac{\Delta\theta_{r\_\text{actual}(k)} - \Delta\theta_{r\_\text{error}(k)}}{\Delta t_s}\end{aligned} \tag{7}$$

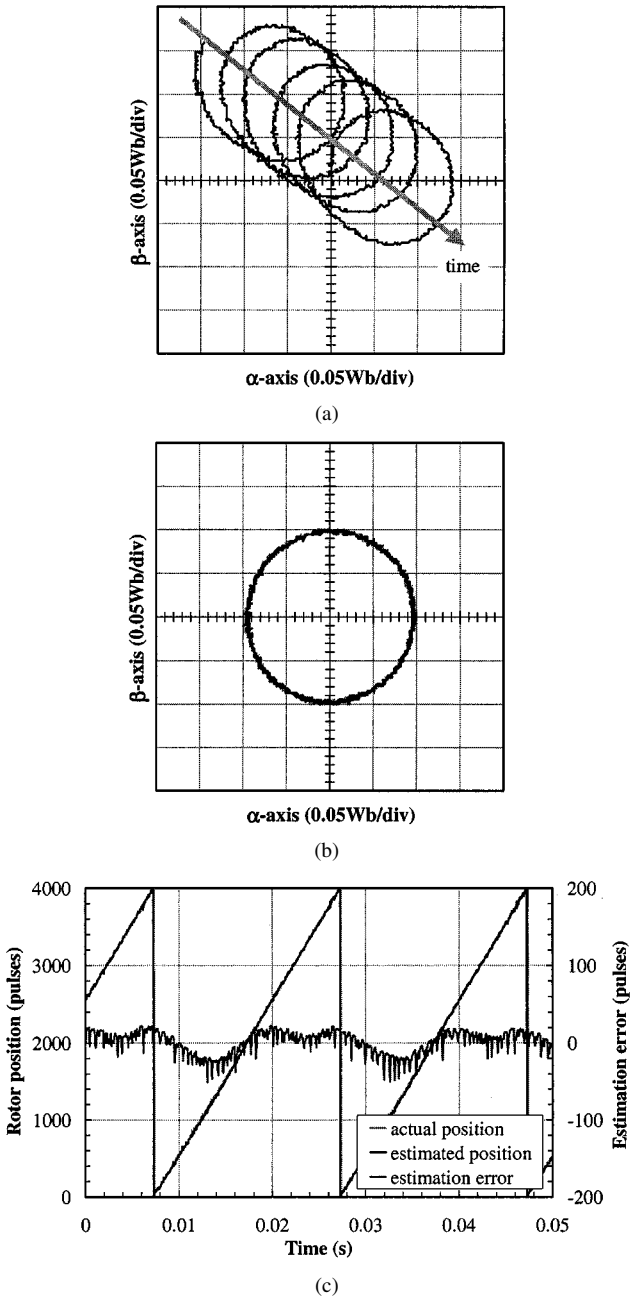

Fig. 3. Results from flux-observer-based position estimation. (a) Locus of observed excitation flux-linkage vector, without high-pass filter. (b) Locus of observed excitation flux-linkage vector, with high-pass filter. (c) Comparison of actual and estimated rotor position, with high-pass filter but without flux filter, 3000 r/min.

where $\theta_{r\_\mathrm{actual}}$ is the actual rotor position and $\theta_{r\_\mathrm{error}}$ is a position error. Although $\theta_{r\_\mathrm{error}}$ may be very much smaller than the range of $\theta_{r\_\mathrm{actual}}$ (i.e., 4000 pulses), $\Delta\theta_{r\_\mathrm{actual}}$ is small since Δt_s is very short. Therefore, $\Delta\theta_{r\_\mathrm{error}}$ may be comparable with $\Delta\theta_{r\_\mathrm{actual}}$, and cause a significant error in the estimated speed. If the motor speed is n r/min, $\Delta\theta_{r\_\mathrm{actual}} = n/60 \times \Delta t_s \times 4000$ pulses. Since $\Delta t_s = 3$ ms in the experimental system, the speed is calculated as $n = 5 \times \Delta\theta_{r\_\mathrm{actual}}$ r/min. Thus, if the actual speed is 3000 r/min, $\Delta\theta_{r\_\mathrm{actual}}$ is 600 pulses. However, from Fig. 3(c) it is seen that $\theta_{r\_\mathrm{error}}$ can be ~50 pulses. Hence, the error in the estimated speed may be 250 r/min, or ~8%. Clearly,

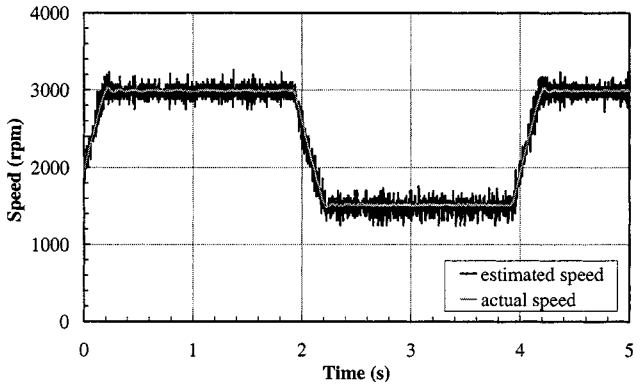

Fig. 4. Derivation of speed from the differential of estimated rotor position.

the error may be much higher at lower speeds, when $\Delta\theta_{r\_\mathrm{error}}$ may be more comparable with $\Delta\theta_{r\_\mathrm{actual}}$.

While the error could be reduced by increasing the sampling time interval Δt_s, this would compromise the dynamic response of the speed estimation, and is not an acceptable solution.

In order to demonstrate the limited performance of this speed estimation method, the commanded speed of the experimental drive was changed from 1500 to 3000 r/min every 2 s, a fuzzy logic algorithm being employed for speed control [16]. The encoder output was used for the vector control, as well as for the measurement of the actual speed for the speed control system. In addition, the rotor position was estimated as described in Section II, and the speed was estimated from the differential of the estimated rotor position. Fig. 4 shows that the estimated speed contains significant ripple, and would be inappropriate for speed feedback in a sensorless drive system.

IV. Filtering of Observed Flux Vector

The ripple which results when the speed is derived from the rotor position is caused by rotor position errors, which arise from noise in the observed flux-linkage vector locus, as in Fig. 3(b). However, Lagerquist [10] proposed that the speed ripple might be reduced significantly by filtering the observed flux vector with a low-pass filter. Thus, this was also implemented in the experimental drive system, in which the excitation flux linkage was observed every 50 μs, the time constant in the transfer function of the low-pass filter, i.e., $1/(Ts+1)$, being set at $T = 500\,\mu$s. The loci of the flux-linkage vector both with and without the filter are shown in Fig. 5. Although the flux filter improves the estimation of the flux-linkage vector locus, an error still exists in the estimated rotor position, as shown in Fig. 5(c). As will be seen, there is a steady-state error of around 100 pulses, or 9° electrical due to the phase shift introduced by the low-pass filter, as is also evident in Fig. 5(c) and (d). This can compromise the vector control performance, especially when the motor is running at high speed. By way of example, Fig. 5(e) shows the influence of the flux filter on the estimated speed, from which it will be evident that the addition of the filter is less effective when the motor runs at high speed, even when its time constant was increased from 125 μs to 2 ms. This is due to low-frequency

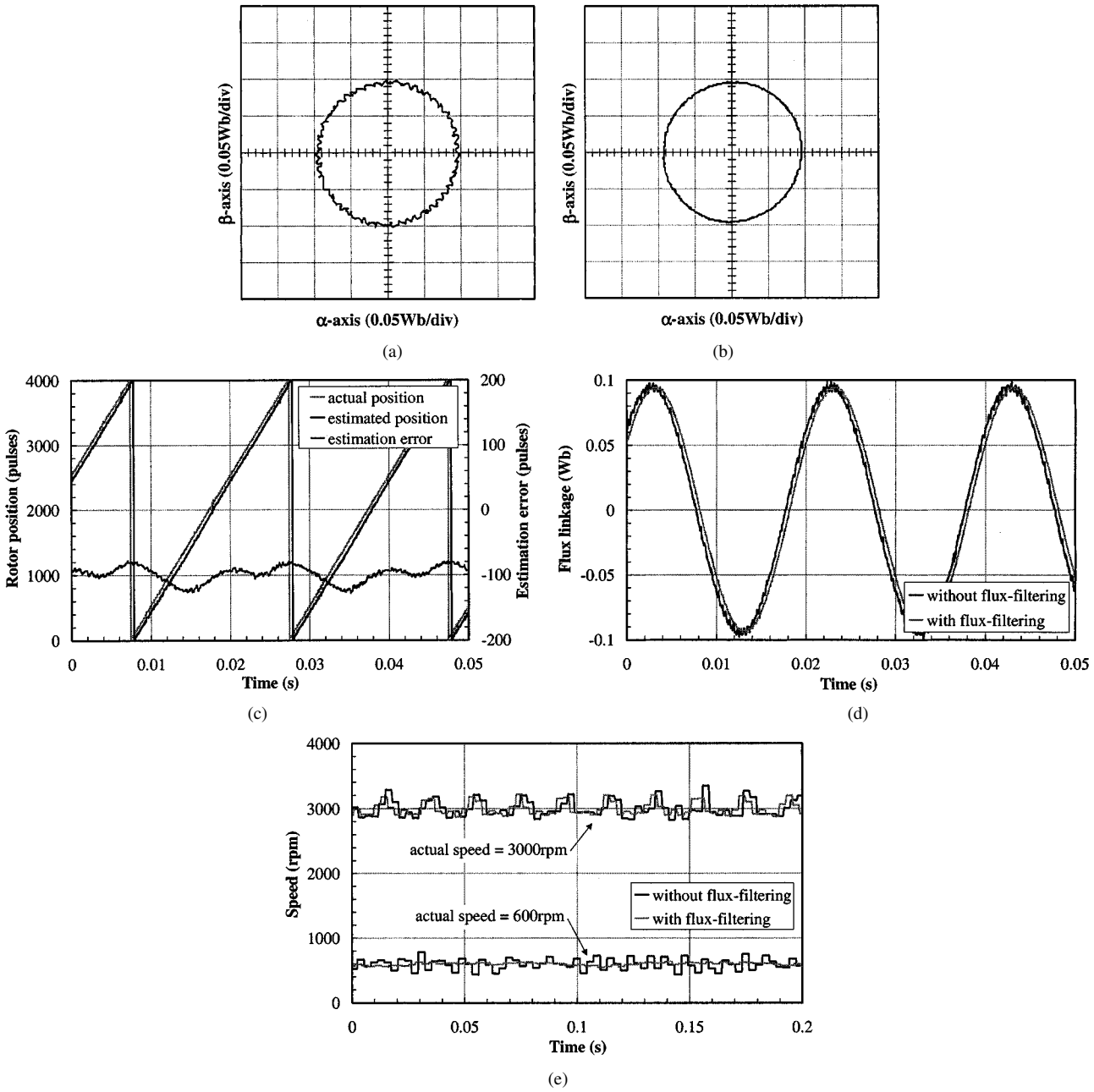

Fig. 5. Influence of low-pass filter on observed flux-linkage vector. (a) Locus of observed flux-linkage vector without flux filter, 3000 r/min. (b) Locus of observed flux-linkage vector with flux filter, 3000 r/min. (c) Comparison of actual and estimated rotor position, with flux filter, 3000 r/min. (d) Observed fluxes ($\psi_{f\alpha}$), with and without flux filter, 3000 r/min. (e) Speed estimation with and without flux filter, 3000 and 600 r/min.

variations in the position error, shown in Figs. 3(c) and 5(c), which are caused by the periodic variation of the motor parameters (such as the change in inductance due to saturation) and thus have a frequency which is comparable with the fundamental flux vector, and which cannot be eliminated by the flux filter. Moreover, the amplitude of the low-frequency components is approximately proportional to the armature current. Thus, the position error and speed error become more significant when the load torque is increased.

In summary, filtering of the observed flux vector may introduce a significant phase shift, and be ineffective in reducing the speed error at high speed. Furthermore, as will be seen in the next section, the flux filter has relatively little effect on improving the estimated average speed.

V. Average Speed Estimation

Since a flux filter is not always effective in reducing the speed error, another low-pass filter is employed to filter the speed, ω_p, derived from the differential of the estimated rotor position, so as to obtain the average speed, ω_d. In the experimental drive system, the speed ω_p was estimated every 3 ms and the time constant of the speed filter was set at 30 ms, much higher than the time constant of the flux filter, such that the speed errors existing in (7) can be reduced significantly. Fig. 6 shows that, when speed filtering was employed, the flux filter had very little influence on the derived average speed, which was very close to the actual steady-state speed.

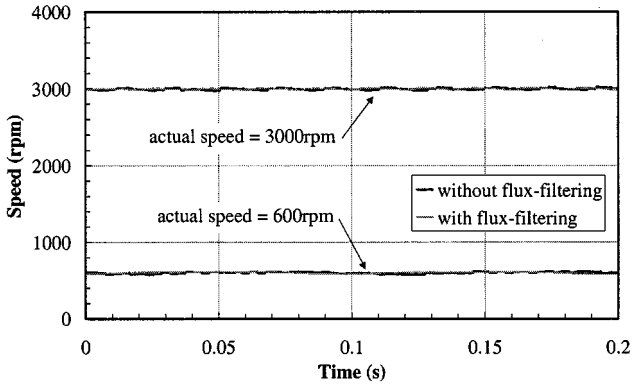

Fig. 6. Influence of flux filter on estimated average speed when low-pass speed filter is employed, 3000 and 600 r/min.

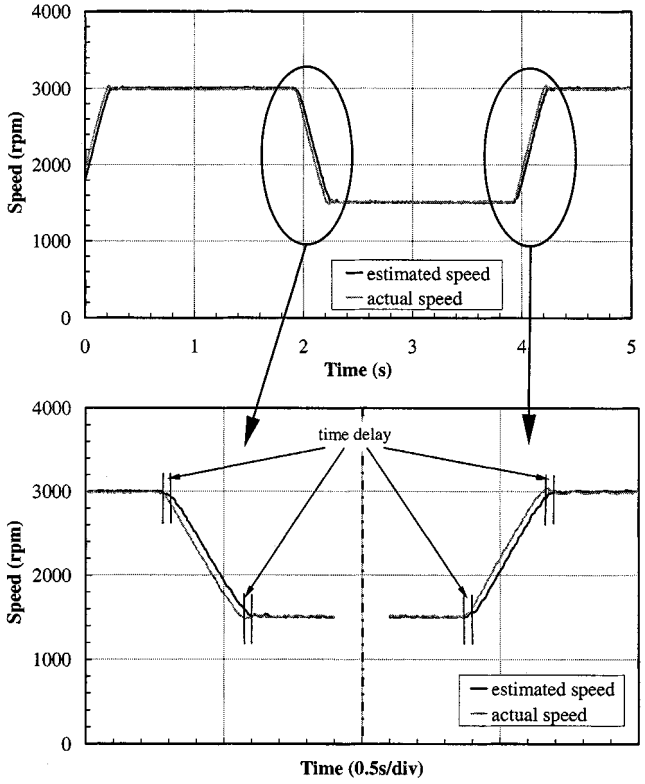

Fig. 7. Average speed estimation.

The experimental procedure which was described earlier to obtain Fig. 4 was again implemented, and the estimated average speed ω_d was compared with the actual speed, as shown in Fig. 7, from which it will be seen that ω_d is in close agreement with the actual speed under steady-state operating conditions. However, it will also be observed, in the lower section of Fig. 7, that there is a noticeable time delay in the estimated speed.

In general, the predicted average steady-state speed is accurate, and unlike the flux filter, the speed filter does not introduce a phase shift in the observed flux-linkage vector. However, since it causes a time delay in the estimated speed, it may compromise the dynamic response of a drive. Thus, this method of speed estimation may also be unsuitable for speed feedback in servo controlled drives.

VI. Speed Estimation From Induced EMF and Excitation Flux Linkage

If the excitation flux linkage is known *a priori* and the amplitude of the induced EMF (E_m) is deduced from the measured current and voltage, then since the two are related in the rotor d–q reference frame by

$$\begin{cases} E_m = \omega\Psi_f \\ u_q = Ri_q + L_s \cdot pi_q + \omega L_s i_d + E_m \end{cases} \tag{8}$$

where $L_s = L_d = L_q$ is the stator winding inductance, assuming a surface-mounted magnet rotor, the speed may be estimated from

$$\omega = \frac{u_q - Ri_q - L_s \cdot pi_q - \omega L_s i_d}{\Psi_f} = \frac{u_q - Ri_q - L_s \cdot pi_q}{\Psi_f + L_s i_d}. \tag{9}$$

The main merit of estimating the speed in this way is that it leads to a fast response. In the experimental drive system, it was estimated every 50 μs, the same frequency as the rotor position estimation. However, it has two significant drawbacks. Firstly, the parameters R, L_s, and Ψ_f are sensitive to variations in temperature and saturation, and although Kim [14] compensated for such parameter variations, this is difficult to implement, as mentioned earlier. Secondly, the speed estimation still involves a differential operation. Thus, for a surface-mounted magnet motor, for which the winding inductance is usually relatively small, and the phase currents may contain a significant ripple, the differential operation can cause a significant error in the estimated speed. This is evident in Fig. 8(a), which shows the d- and q-axes currents (i_d and i_q), calculated from the measured phase currents, when the motor speed was changed from 1500 to 3000 r/min, as described earlier.

Since the estimation of speed from the induced EMF and excitation flux linkage is inherently inaccurate, a further variant, *viz.* eliminating the differential operation in (9), has been investigated so as to simplify the calculation. While this increases the potential for error in the estimated speed, it ensures fast response. Moreover, since, in a surface-mounted magnet motor, $L_s i_d$ is usually much smaller than Ψ_f, especially when the d-axis current reference is set to zero in the vector control, (9) may be simplified to

$$\omega_e \approx \frac{u_q - Ri_q}{\Psi_f}. \tag{10}$$

Since noise in i_q can still cause a ripple in the estimated speed, a low-pass filter, with a time constant of 2.5 ms, was applied to the numerator of (10). It does not significantly compromise the dynamic performance since its time constant is relatively small. The motor speed was again varied from 1500 to 3000 r/min every 2 s, the encoder being used for both vector control and speed control, while the speed was also estimated from (10) and compared with the actual speed, as shown in Fig. 8(b). It can be seen that the response of the estimated speed change is fast, which is the most important feature of the method, although the accuracy of the estimation is not good.

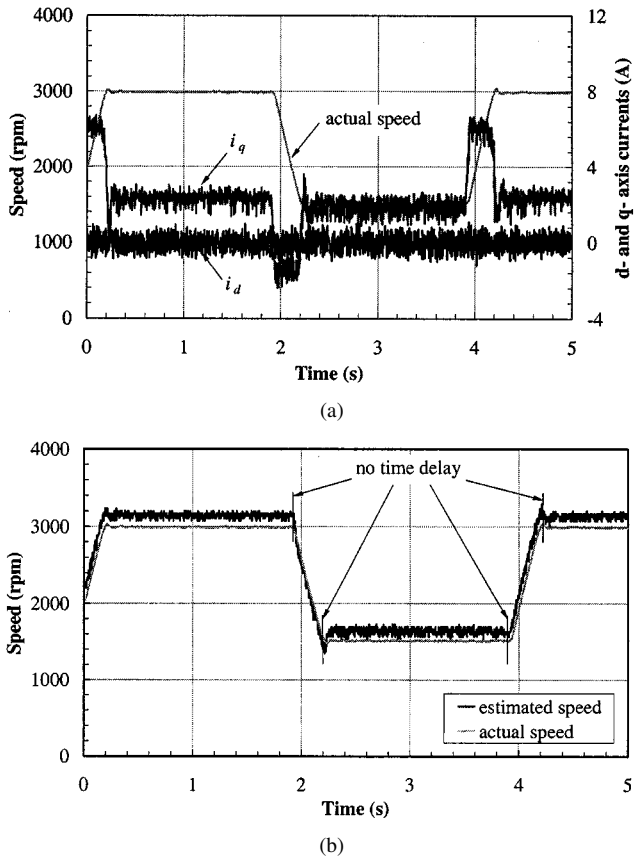

Fig. 8. Estimation of speed from EMF and excitation flux. (a) d-axis and q-axis currents, rich of noise. (b) Comparison of estimated and actual speed.

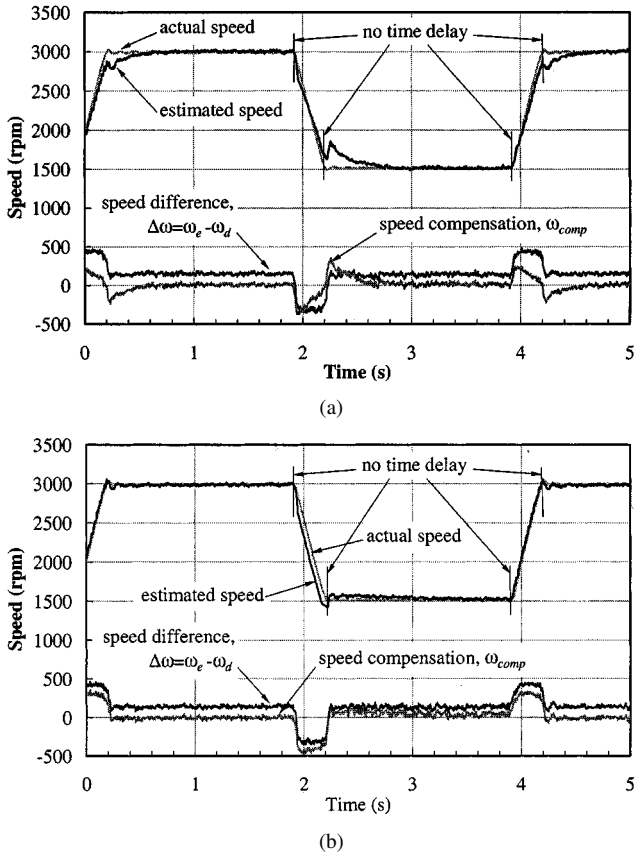

Fig. 9. Performance of improved speed estimation method. (a) Time constant $T = 10$ s. (b) Time constant $T = 100$ s.

VII. Improved Method of Speed Estimation

From the results presented in Figs. 7 and 8, the following conclusions can be drawn: 1) a phase difference exists between the estimated average speed, ω_d, derived from the differential of the estimated rotor position and the actual speed and 2) a magnitude error exists between the actual speed and the estimated speed, ω_e, derived from the induced EMF and excitation flux-linkage. Thus, neither method is entirely suitable for speed feedback. However, the two methods can be combined to improve the estimation of the speed.

The following improved estimation of rotor speed, ω_h, is proposed:

$$\omega_h = \omega_d \frac{1}{Ts+1} + \omega_e \frac{Ts}{Ts+1}. \tag{11}$$

If $s \to 0$, then $\omega_h \to \omega_d$. Thus, under steady-state operation, ω_d plays the dominant role in the speed estimation. However, if $s \to \infty$, then $\omega_h \to \omega_e$. Hence, under transient conditions, ω_e plays the dominant role. Equation (11) can be re-expressed as

$$\omega_h = \omega_d + (\omega_e - \omega_d)\frac{Ts}{Ts+1} = \omega_d + \Delta\omega \frac{Ts}{Ts+1} = \omega_d + \omega_{\text{comp}}. \tag{12}$$

Thus, the proposed speed estimation method compensates the average speed ω_d by adding ω_{comp}, where ω_{comp} is the output of the high-pass filtering of $\Delta\omega = \omega_e - \omega_d$.

The performance of the proposed method was again assessed experimentally, by changing the commanded speed from 1500 to 3000 r/min, as before. The variations of ω_e and ω_d were shown earlier in Figs. 8(b) and 7, while their difference, $\Delta\omega$, is shown in Fig. 9. During the time interval from 0.2 to 4.2 s, there are two steady-state operating periods, *viz.*, between 0.2–1.9 s and between 2.2–3.9 s, and two transient periods, *viz.*, between 1.9–2.2 s and between 3.9–4.2 s. Clearly, during the steady-state periods, there should be no error in ω_h. However, during the transient periods, a small error in ω_h is acceptable if ω_h can follow the change in the actual speed. Therefore, it is desirable that the speed compensation ω_{comp} is zero under steady-state conditions, and approaches $\Delta\omega$ under transient conditions. To achieve this, an appropriate value for the time constant T of the high-pass filter must be selected. Since it is difficult to calculate T analytically, it is determined experimentally simply by modifying the DSP program and observing the system performance.

As will be seen from Fig. 9, irrespective of the time constant T, $\Delta\omega$ is nearly constant (150 r/min) during the steady-state period from 0.2 to 1.9 s. Thus, ω_{comp}, the output of the high-pass filtering of $\Delta\omega$, is zero by the end of this period. $\Delta\omega$ is also nearly constant (-300 r/min) during the transient period from 1.9 s to 2.2 s. Therefore, at the beginning of this transient period, the step change in $\Delta\omega$ from 150 to -300 r/min results in a value for -450 r/min in ω_{comp}, i.e., an overcompensation in the estimated speed ω_h. In other words, as soon as the actual speed decreases, ω_h also decreases without a time delay. Although there is an error in ω_h due to the overcompensation, it

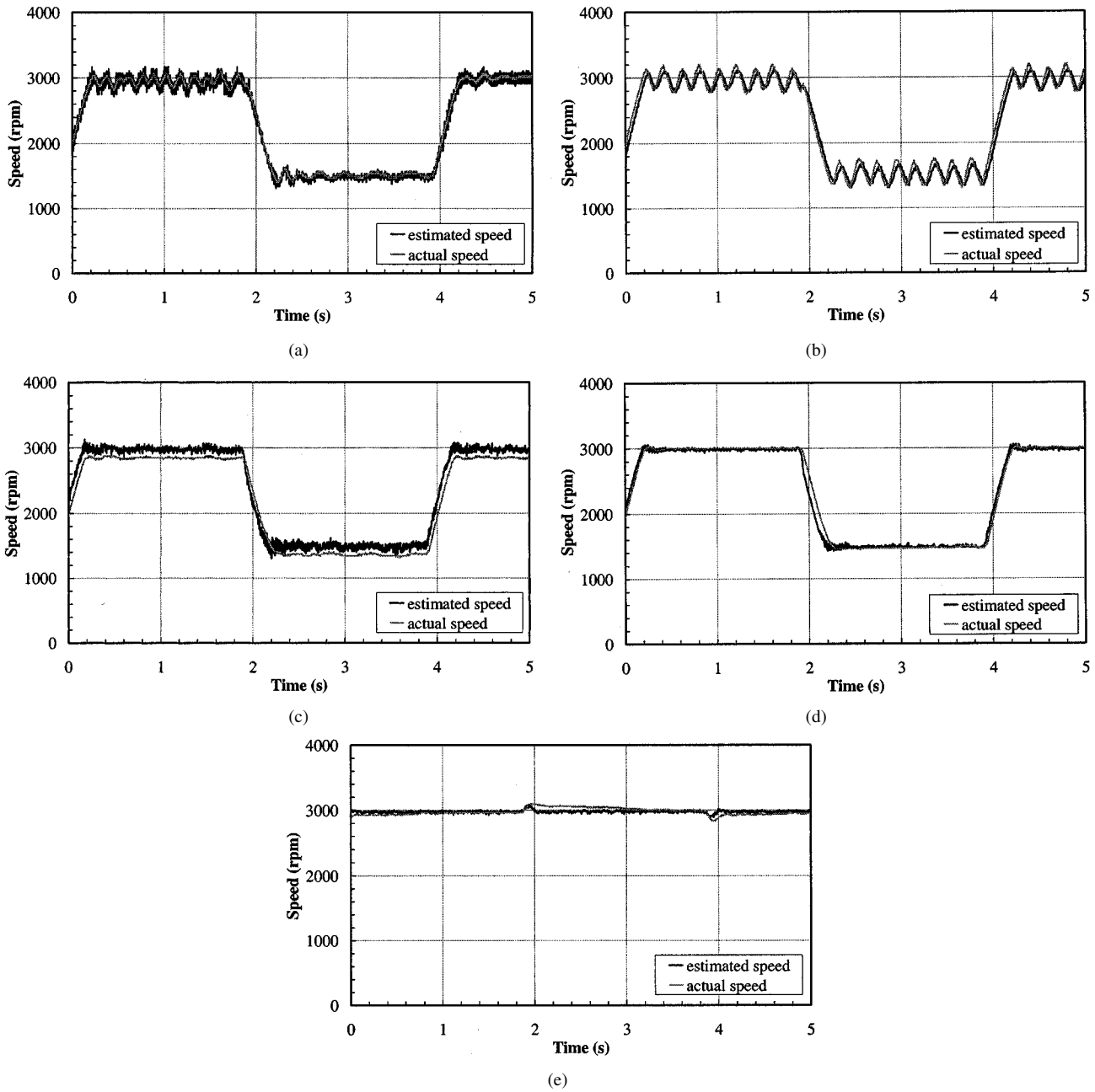

Fig. 10. Speed control performance with different sensorless speed feedback methods. (a) Speed feedback derived from differential of estimated rotor position (ω_p), changing speed command. (b) Speed feedback using estimated average speed (ω_d), changing speed command. (c) Speed feedback derived from EMF and excitation flux linkage (ω_e), changing speed command. (d) Speed feedback using improved method of speed estimation (ω_h), changing speed command. (e) Speed feedback using improved method of speed estimation (ω_h), 3000 r/min, changing load torque.

is not critical since ω_h reflects the change in the actual speed. However, when the time constant T is set to a small value, such as 10 s, $\omega_{\rm comp}$ decreases quickly from -450 r/min and unexpectedly reaches zero during the transient period [Fig. 9(a)], such that the speed compensation disappears and ω_h is considerably in error from the actual speed. Moreover, between this transient period and the next steady-state period, a step change in $\Delta\omega$ from -300 to 150 r/min occurs, which results in an increase of 450 r/min in $\omega_{\rm comp}$. Thus, ω_h is overcompensated, and is further from the actual speed. During the steady-state period from 2.2 to 3.9 s, however, $\omega_{\rm comp}$ decreases from 450 r/min to zero, and ω_h becomes equal to the actual speed. Consequently, as can be seen, a significant error exists in the estimated speed at the beginning of each steady-state operating period, and this will compromise the system performance. However, when the time constant T is increased, to 100 s, $\omega_{\rm comp}$ only gradually decreases from -450 r/min during the transient period from 1.9 to 2.2 s, becoming -400 r/min by the end of this period (Fig. 9(b)), thus, the overcompensation is always effective, and an error in ω_h is always noticeable. However, this error is not critical, since ω_h correctly reflects the change in the actual speed. Similarly, between this transient period and the following steady-state period, $\omega_{\rm comp}$ increases by 450 r/min, its value becoming 50 r/min. Therefore, ω_h is now only slightly overcompensated, and is very close to the actual speed. Moreover, during the steady-state period from 2.2 to 3.9 s, $\omega_{\rm comp}$ decreases quickly from 50 r/min

to zero, when ω_h corresponds to the actual speed. In summary, errors in the estimated speed at the beginning of each steady-state operating period can be significantly reduced by choosing an appropriate time constant T, and the estimated speed by the proposed method agrees well with the actual speed, especially during steady-state operation. Thus, it can be employed for speed feedback in a sensorless drive system.

VIII. Sensorless Speed Control

In order to demonstrate the performance of the four methods of speed estimation which have been considered when they are employed in a closed-loop speed-controlled brushless drive, the load torque was maintained constant while the commanded speed was varied between 1500–3000 r/min every 2 s, fuzzy logic control being employed for the speed control. The drive was the same as that which was used to obtain the results shown in Figs. 4 and 7–9, except that the estimated speed (i.e., ω_p, ω_d, ω_e, and ω_h) is now employed for speed feedback rather than the actual speed as in the previous tests.

As will be seen in Fig. 10(a), when the speed feedback was derived from the differential of the estimated rotor position, the speed exhibited a significant high-frequency oscillation as well as a low-frequency ripple, while when the estimated average speed was employed as feedback (Fig. 10(b)) the speed was unstable. When the speed feedback was derived from the induced EMF and excitation flux linkage, although the dynamic response was good, a speed error as well as a small speed ripple existed during steady-state operation, as will be seen in Fig. 10(c). However, when the proposed method of speed estimation was employed as speed feedback, the steady-state speed error was very small, and the dynamic response was good, as shown in Fig. 10(d).

In a further test to demonstrate the performance of the proposed method of speed estimation, the commanded speed was set at 3000 r/min, and the load torque was switched on and off every 2 s. As will be seen in Fig. 10(e), the dynamic and steady-state speed errors were very small.

IX. Conclusions

Various methods for estimating the speed of a sensorless BLAC motor drive have been implemented and compared. Although the estimation of the average speed from the differential of the rotor position is adequate for steady-state operation, phase delay compromises the system dynamic performance. In contrast, while the estimation of the speed from the EMF and excitation flux linkage has a fast response, the steady-state performance is compromised by the ripple and error in the estimated speed. The proposed method of speed estimation combines the best features of the average speed estimation and the EMF and flux-based estimation methods, and has been shown to yield improved performance. It is, therefore, eminently suitable for closed-loop speed control.

References

[1] M. H. Park and H. H. Lee, "Sensorless vector control of permanent magnet synchronous motor using adaptive identification," in *Proc. IEEE IECON'89*, 1989, pp. 209–214.

[2] V. Sadasivam and L. Xu, "A robust position sensorless vector control of permanent magnet machines by torque angle estimation," in *Proc. IEEE Int. Conf. Power Electronics and Drives System*, 1997, pp. 524–529.

[3] K. Tatematsu, D. Hamada, K. Uchida, S. Wakao, and T. Onuki, "Sensorless control for permanent magnet synchronous motor with reduced order observer," in *Proc. IEEE PESC'98*, 1998, pp. 125–131.

[4] N. Matsui and M. Shigyo, "Brushless DC motor control without position and speed sensor," *IEEE Trans. Ind. Applicat.*, vol. 28, pp. 120–127, Jan./Feb. 1992.

[5] N. Matsui, "Sensorless PM brushless DC motor drives," *IEEE Trans. Ind. Electron.*, vol. 43, pp. 300–308, Apr. 1996.

[6] T. H. Liu and C. P. Cheng, "Controller design for a sensorless permanent-magnet synchronous drive system," *Proc. Inst. Elect. Eng.*, pt. B, vol. 140, pp. 369–378, Nov. 1993.

[7] T. Senjyu, T. Shimabukuro, and K. Uezato, "Vector control of permanent magnet synchronous motors without position and speed sensors," in *Proc. IEEE PESC'95*, 1995, pp. 759–765.

[8] L. Xu and C. Wang, "Implementation and experimental investigation of sensorless control schemes for OMSM in super-high variable speed operation," in *Conf. Rec. IEEE-IAS Annu. Meeting*, 1998, pp. 483–489.

[9] D. Yousfi, M. Azizi, and A. Saad, "Position and speed estimation with improved integrator for synchronous motor," in *Proc. IEEE IECON'99*, vol. 3, 1999, pp. 1097–1102.

[10] R. Lagerquist, I. Boldea, and T. J. E. Miller, "Sensorless control of the synchronous reluctance motor," *IEEE Trans. Ind. Applicat.*, vol. 30, pp. 673–682, May/June 1994.

[11] H. Watanabe, S. Miyazaki, and T. Fujii, "Improved variable speed sensorless servo system by disturbance observer," in *Proc. IEEE IECON'90*, 1990, pp. 40–45.

[12] S. M. A. Sharkh and V. Barinberg, "A new approach to rotor position estimation for a PM brushless motor drive," in *Proc. 9th Mediterranean Electrotechnical Conf.*, 1998, pp. 1199–1203.

[13] ——, "Design and performance of a new technique for sensorless control of a downhole brushless PM motor," in *Proc. IEE Power Electronics and Variable Speed Drives Conf.*, 1998, pp. 263–268.

[14] J. S. Kim and S. K. Sul, "New approach for high-performance PMSM drives without rotational position sensors," *IEEE Trans. Power Electron.*, vol. 12, pp. 904–911, Sept. 1997.

[15] H. Tajima and Y. Hori, "Speed sensorless field-orientation control of the induction machine," *IEEE Trans. Ind. Applicat.*, vol. 29, pp. 175–180, Jan./Feb. 1993.

[16] J. X. Shen, Z. Q. Zhu, and D. Howe, "Hybrid PI and fuzzy logic speed control of PM brushless AC drives," in *Proc. 9th European Conf. Power Electronics and Applications*, 2001, CD ROM.

J. X. Shen (M'98) was in born in Zhejiang Province, China, in 1969. He received the B.Eng. and M.Eng. degrees from Xi'an Jiaotong University, Xi'an, China, in 1991 and 1994, respectively, and the Ph.D. degree from Zhejiang University, Hangzhou, China, in 1997, all in electrical engineering.

From 1997 to 1999, he was a Post-Doctoral Fellow at Nanyang Technological University, Singapore. Since 1999, he has been with the Department of Electronic and Electrical Engineering, University of Sheffield, Sheffield, U.K. His current research interests include designs and applications of permanent-magnet machines and drives, sensorless controls, ultrahigh-speed motors, and fuzzy logic controls.

Z. Q. Zhu (M'90–SM'00) received the B.Eng. and M.Sc. degrees from Zhejiang University, Hangzhou, China, in 1982 and 1984, respectively, and the Ph.D. degree from the University of Sheffield, Sheffield, U.K., in 1991, all in electrical and electronic engineering.

From 1984 to 1988, he lectured in the Department of Electrical Engineering, Zhejiang University. Since 1988, he has been with the University of Sheffield, where he is currently a Professor of Electronic and Electrical Engineering. His current major research interests include applications, control, and design of permanent-magnet machines and drives.

Prof. Zhu is a Chartered Engineer in the U.K. and a member of the Institution of Electrical Engineers, U.K.

David Howe received the B.Tech. and M.Sc. degrees from the University of Bradford, Bradford, U.K., in 1966 and 1967, respectively, and the Ph.D. degree from the University of Southampton, Southampton, U.K., in 1974, all in electrical power engineering.

He has held academic posts at Brunel and Southampton Universities and spent a period in industry with NEI Parsons Ltd., working on electromagnetic problems related to turbo-generators. He is currently a Professor of Electrical Engineering at the University of Sheffield, Sheffield, U.K., where he heads the Electrical Machines and Drives Research Group. His research activities span all facets of controlled electrical drive systems, with particular emphasis on permanent-magnet excited machines.

Prof. Howe is a Chartered Engineer in the U.K. and a Fellow of the Institution of Electrical Engineers, U.K.